$Ba_{2-x}Sr_xCuO_2CO_3$: A Series of Oxycarbonate Thin Films Grown by Pulsed Laser Deposition on $NdGaO_3$ Substrates

W. Prellier,* A. Tebano,† J. L. Allen, J. F. Hamet, B. Mercey, M. Hervieu, and B. Raveau

Laboratoire CRISMAT-ISMRA et Université de Caen, Bd du Maréchal Juin 14050, Caen Cedex, France

Received July 17, 1996. Revised Manuscript Received September 27, 1996[⊗]

Monophasic thin films of the oxycarbonates $Ba_{2-x}Sr_xCuO_2CO_3$ have been grown by pulsed laser deposition on [110]-oriented $NdGaO_3$ substrates for $x = 2$, 1.6, 0.9, 0.4, and 0.3. A systematic study of these films by X-ray diffraction and transmission electron microscopy shows that the film orientation varies from *a*-axis or [110] orientation (copper layers perpendicular to the substrate) to a *c*-axis or [001] orientation (copper layers parallel to the substrate) as *x* decreases. $Sr_2CuO_2CO_3$ ($x = 2$) is indeed *a*-axis oriented, whereas for $0.4 < x < 1.6$ these films have a [110] orientation, and finally for $x = 1.6-1.7$ the films exhibit *c*-axis, [110]- and [1$\bar{1}$0]-oriented domains. The factors which influence the orientation of these films are discussed.

Introduction

The recent synthesis of thin films of oxycarbonates $(CaCuO_2)_m(Ba_2CuO_2CO_3)_n$ by pulsed laser deposition (PLD)[1,2] is of high interest since it is the first time that superconductors with a T_c ($R = 0$) of 75 K, containing only "BaCaCu" have been deposited as thin films. But most important is the fact that the resistance curves of such films show a broad transition with a T_c(onset) of 110 K, i.e., significantly larger than that observed for $YBa_2Cu_3O_{7-\delta}$ which has been studied as a thin film.[3,4] High-resolution electron microscopy of the PLD thin films of $(CaCuO_2)_m(Ba_2CuO_2CO_3)_n$ shows that they are far from optimized: several members coexist within the same film and 90° oriented domains are systematically formed.[2] These results strongly suggest that it should be possible to deposit oxycarbonate thin films with a zero resistance at 110 K, provided the growth of the different members of this series and their preferential axis orientation can be carefully controlled. For this reason, we have recently undertaken the study of the deposition of the first member ($m = 0$; $n = 1$) of the series, showing that it is possible to grow thin films containing a single member with composition $Ba_{1.8}Ca_{0.2}CuO_2CO_3$ and $Ba_{1.6}Sr_{0.4}CuO_2CO_3$.[5] Thus herein we report on the systematic study of the PLD of the oxycarbonate $Ba_{2-x}Sr_xCuO_2CO_3$ (abbreviated hereafter BSCC) whose structure (Figure 1a) consists of single perovskite layers interconnected with rows of CO_3 groups. We show that a monophasic thin film ($m = 0$; $n = 1$), can be deposited for $0.3 \leq x \leq 2$, whose

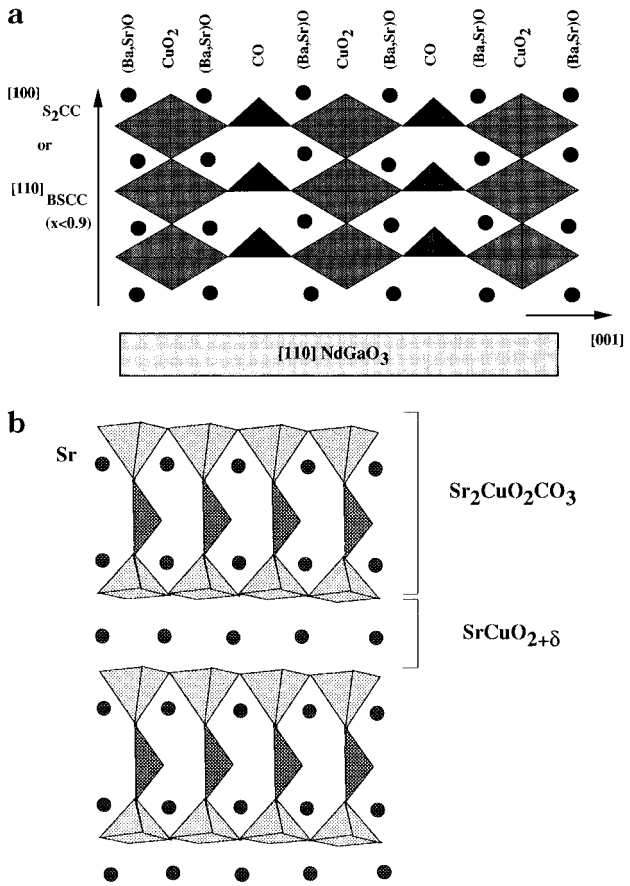

Figure 1. (a) Schematic representation of the structure of the oxycarbonate $Ba_{2-x}Sr_xCuO_2CO_3$, [100] oriented for $x = 2$ (S_2CC), and [110] oriented for $x < 0.9$, on $NdGaO_3$. Triangles represent the carbonate groups. (b) Idealized drawing of the member ($m = 1$, $n = 1$) of the family $(SrCuO_{2+\delta})_m(Sr_2CuO_2CO_3)_n$.

† INFM-Dipartimento di Ingegneria Meccanica, Università di Roma "Tor Vergata", via della Ricerca Scientifica, 00133, Roma, Italy

⊗ Abstract published in *Advance ACS Abstracts,* December 1, 1996.

(1) Allen, J. L.; Mercey, B.; Prellier, W.; Hamet, J. F.; Hervieu, M.; Raveau, B. *Physica C* **1995**, *241*, 158.

(2) Hervieu, M.; Mercey, B.; Prellier, W.; Allen, J. L.; Hamet, J. F.; Raveau, B. *J. Mater. Chem.* **1996**, *6*, 165.

(3) Dijkkamp, D.; Verkatesan, T.; Wu, X. D.; Shaheen, S. A.; Jinawi, N.; Minke-Lee, Y. H.; McLean, W. L.; Crogt, M. *Appl. Phys. Lett.* **1987**, *51*, 619.

(4) Fröhlingsdorf, J.; Zander, W.; Stritzker, B. *Solid State Commun.* **1988**, *67*, 1557.

(5) Prellier, W.; Tebano, A.; Allen, J. L.; Hamet, J. F.; Mercey, B.; Hervieu, M.; Raveau, B. *Chem. Mater.*, press.

S0897-4756(96)00378-X CCC: $14.00

orientation with respect to the substrate varies with the strontium content.

Experimental Section

Five targets of nominal compositions Sr_2CuO_3, $Ba_{0.4}Sr_{1.6}CuO_3$, $Ba_{1.1}Sr_{0.9}CuO_3$, $Ba_{1.6}Sr_{0.4}CuO_3$, and $Ba_{1.9}Sr_{0.1}CuO_3$ were prepared by solid-state reaction, starting from $BaCO_3$, $SrCO_3$, and CuO. The well-ground mixtures were calcined at 650 °C for 10 h. After grinding, the resultant was fired at 800 °C. Heatings were done in a tube furnace in air. The powders were ground again and pressed into a pellet which was sintered around 950 °C. A pulsed KrF excimer laser (Lambda Physik LPX200, $\lambda = 248$ nm) was used to deposit films from the target onto the [110]-oriented $NdGaO_3$ (NGO) substrates. The crystallographic structure of $NdGaO_3$ is orthorhombic with $a = 5.426$ Å, $b = 5.502$ Å, and $c = 7.706$ Å.

The fluence was adjusted to 2 J/cm^2 and the rate to 5 Hz. Substrate temperature, deposition pressure, and posttreatment were systematically varied. The best results were obtained for a temperature of 680 °C and partial pressures of 0.15 mbar for O_2 and 0.05 mbar for CO_2 followed by a slow cool down to room temperature, in 500 mbar of the same gas mixture. For each of these compositions, varying the temperature leads to a complete decomposition of the phase. This means that it is not possible to change the film orientation by increasing the substrate temperature. The typical film thicknesses are about 3000 Å.

The structural study has been carried out by X-ray diffraction using a Seifert XRD 300 diffractometer with Cu $K\alpha_1$ radiation ($\lambda = 1.5405$ Å) for the $\theta-2\theta$ measurements. Transmission electron microscopy (TEM) was performed with a JEOL 200 CX microscope and high-resolution electron microscopy (HREM) with a TOPCON 002B, having a point resolution of 1.8 Å. Each microscope is equipped with an energy-dispersive scattering (EDS) analyzer.

Results and Discussion

Deposition of $Sr_2CuO_2CO_3$(S_2CC) ($x = 2$). *Electron diffraction:* The thin films were investigated systematically coupling EDS and electron diffraction in numerous areas. The EDS analyses attest that the cation composition is almost constant over the whole film, with a slight copper excess with regard to the nominal composition, i.e., the Sr/Cu ratio is close to 1.8. The ED patterns recorded along the direction perpendicular to the substrate are complex. They can be all interpreted considering the superimposition of two different structures directly related to that of the ideal S_2CC cell (Figure 1a) and the systematically superposition of two 90° oriented variants of these structures. The selected area electron diffraction (SAED) patterns of each of the structures are displayed in Figures 2a and 3a; they have been recorded in areas where 90° oriented domains take place but where the two superstructures are not superimposed.

The simplest ED pattern (Figure 2a) can be described from the superimposition of two variants of a tetragonal cell with $a \approx a_p$ (a_p is the parameter of the cubic perovskite, close to 3.9 Å) and $c \approx 2a_p$. The reconstruction of the reciprocal space shows that there is no condition limiting the reflection. The reflections are indexed, using the symbol $\perp$ to marked one of the two variants. The splitting of the spot corresponding to the superposition of the $100_\perp$ and 002 reflections show that the c parameter is slightly shorter that $2a$. This pattern shows also that the $00l$ reflections are elongated along c^*, suggesting the existence of stacking defects along this axis. These cell parameters and symmetry correspond to those of the S_2CC structure reported by Narendra Babu et al.[6] but which are not those usually reported for the bulk material.[7,8]

The ED pattern of the second structural type is given in Figure 3a. The reflection indexation shows that the a and c parameters are doubled with $a \approx 2a_p \approx 7.7$ Å and $c \approx 4a_p \approx 15$ Å. The conditions limiting the reflections are $0kl$; $k + l = 2n$. However, due to the systematically superimposition of the different domains, the rotation about the a^* and c^* axes cannot provide an univocal answer for the cell parameters and symmetry. Two solutions are indeed compatible with the different ED patterns: A 4-fold tetragonal supercell with $a \approx 2a_p \approx 7.7$ Å and $c \approx 4a_p \approx 15$ Å and hkl, $h + k + l = 2n$ i.e., an I-type symmetry. These cell parameters and symmetry are compatible with those usually observed for the bulk sample.[7,8] A 2-fold orthorhombic cell with $a \approx a_p \approx 3.85$ Å, $b \approx 2a_p \approx 7.7$ Å, and $c \approx 4a_p \approx 15$ Å and hkl, $k + l = 2n$, i.e., an A-type symmetry.

90° oriented variants of this system are also clearly observed on the ED pattern; they are indexed in Figure 3a. Note that for the high k and l values, a splitting of the spots is also observed along the two perpendicular directions resulting from the fact that the c length is smaller than $2a$ (15 Å rather than 15.6 Å).

High-resolution electron microscopy: The film morphology and the structure of the two variants were investigated by high-resolution electron microscopy. It appears that they are correlated.

The HREM image recorded for a zone corresponding to the "$a_p \times 2a_p$" structure is given in Figure 2b. It is important to note that in such areas the film consists of very large grains (of the order of the micrometer), each grain being a puzzle of adjacent 90° oriented very small domains, 100 or 200 Å large. The nature of the domain boundaries and defects will be discussed here after. The enlarged images (Figure 2c) recorded in the thinnest parts of the films exhibit clearly the contrast characteristic of the presence of carbonate groups which consists in small grey dots surrounded by four crossed bright dots;[9] they are indicated by a black arrowhead in Figure 2c. In the thicker part of the film, the rows of carbonate groups appear as rows of very bright dots. The stacking along c of alternating copper and carbonate layers, separated by [SrO] layers, confirms the S_2CC structural type of the film. The simulated images, calculated for the positional parameters refined by Babu[6] varying the focus and crystal thickness, confirm this assertion. One example is given in Figure 2d, for $t = 25$ Å.

The HREM image recorded for a zone corresponding to the "$2a_p \times 4a_p$" structure is given in Figure 3b. The difference between the morphologies of the two structures is straightforward in such an image. When the "$2a_p \times 4a_p$" structure is well established, the film exists as small grains, a few hundred angstroms large, and then each of the 90° oriented domains systematically

(6) Babu, T. G. N.; Fish, D. S.; Greaves, C. *J. Mater. Chem.* **1991**, *1*, 677.
(7) Milat, O.; Van Tendeloo, G.; Amelinckx, S.; Babu, T. G. N.; Greaves, C. *J. Solid State Chem.* **1994**, *109*, 5.
(8) Myazaki, Y.; Yamane, H.; Kajitani, T.; Oku, T.; Hiraga, K.; Morii, Y.; Fuchizaki, K.; Funahashi, S.; Hirai, T. *Physica C* **1992**, *196*, 434.
(9) Hervieu, M.; Pelloquin, D.; Michel, C.; Van Tendeloo, G.; Raveau, B. *J. Solid State Chem.* **1994**, *112*, 139.

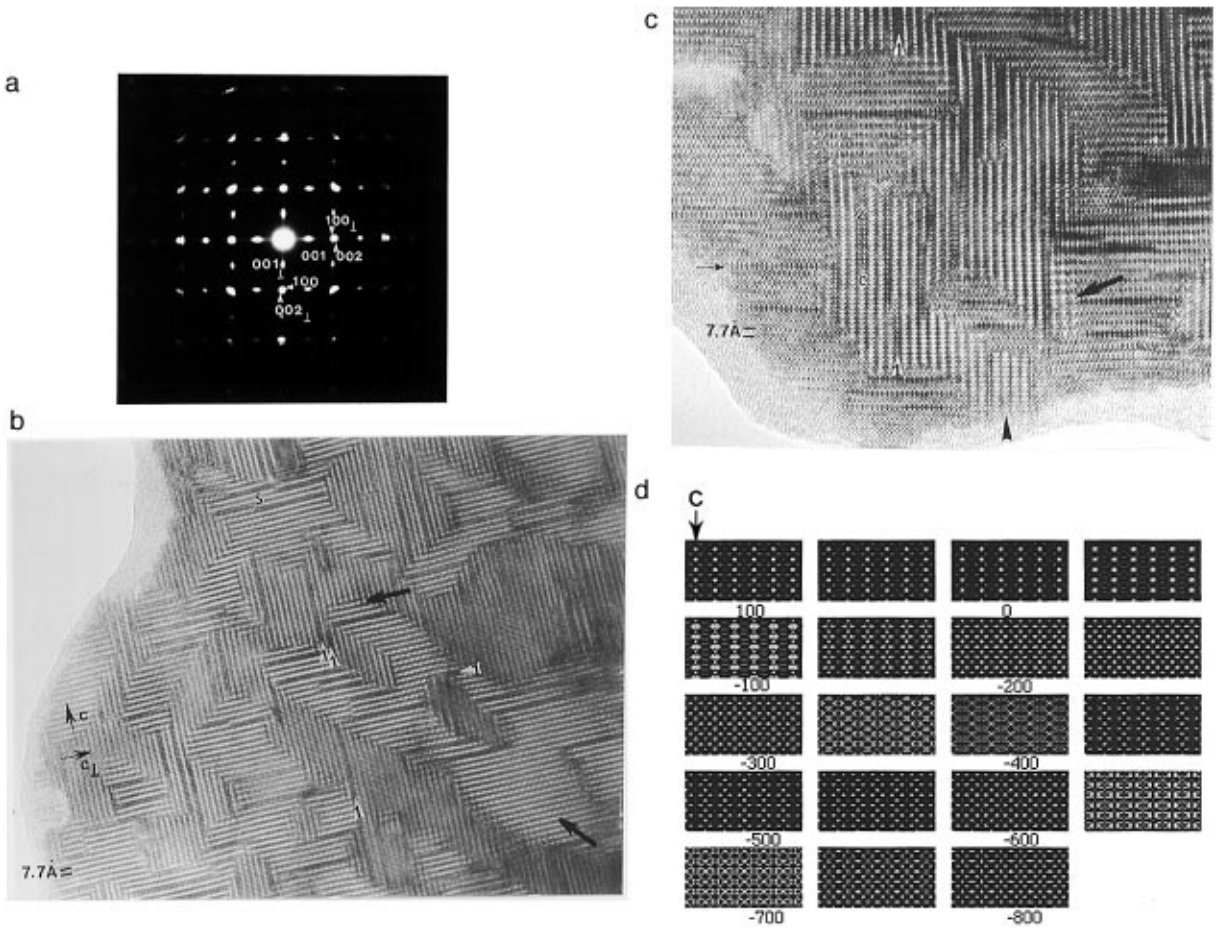

Figure 2. $Sr_2CuO_2CO_3$, first structural type. (a) [010] ED pattern corresponding to the superimposition of two variants of a tetragonal cell "$a_p \times 2a_p$". The reflections are elongated along c^*. (b) Corresponding overall HREM image showing the shape and relative arrangement of the 90° oriented domains. Some of the intergrowth defects, that are the $m = 1$, $n = 1$ members of the family are indicated by black triangles labeled **1**, additional and shearing by **S**. Areas where a centered superstructure is established are shown by large black arrows. (c) Enlarged HREM image. The rows of bright dots surrounded by four crossed bright dots are correlated to the carbonate rows. The intergrowth defects marked **1** and **2** correspond to the members $m = 1$ and 2 of the series and **C** and **S** to layer interconnections. (d) Simulated images calculated for the positional parameters refined by Babu et al.[6] for a thickness $t = 25$ Å. The focus values are given in angstroms.

corresponds to a whole grain. The periodicity along the *b* and *c* parameters and the centering of the contrast is also clearly observed. Very thin areas are hardly observed, even in the crystal edges and the contrast consists of staggered rows of bright dots, 7.7 Å spaced along *b*. To understand the contrast and the structure of these areas, images were simulated considering the tetragonal structure proposed by Miyazaki[8] from XRD and neutron diffraction data (in the space group $I\bar{4}$). The cell parameters, $2a_p \times 4a_p$, and symmetry are correlated, in the bulk oxycarbonates,[7,8] to small atomic displacements and carbonate groups ordering. As expected, the contrast variation arising from such a phenomenon is scarcely visible, whatever the focus values for a crystal thickness up to 70 Å. This is illustrated in Figure 3c, where the through focus series is given for a crystal thickness of 25 Å and in Figure 3d where the variation of the contrast is given vs the thickness for focus values close to −250 Å where the zones of light electron density appear as bright dots. This is also in agreement with the HREM studies carried out by Miyazaki[8] and Milat[7] in the bulk $Sr_2CuO_2CO_3$. To explain the amplitude of the contrast variation at the level of the carbonate layers, the hypothesis of a partial substitution of copper for carbon within the carbonate layers could be considered. The basal ideal structure could be simply described by the alternance of one copper and one carbon along *b* in the so-called carbonate layer, leading to $b \approx 2a_p$, this ordering being translated by a_p (along *b*) in the adjacent carbonate layer leading to a centered structure. Simulated images were calculated on the basis of this structural hypothesis (Figure 3e) considering the ideal positional parameters in the space group *Amm*2. They show that the centered contrast is well generated and that it clearly appears for several focus values. An example is given in Figure 3f for a crystal thickness of 45 Å. These images cannot be considered as those of the actual structure since the exact positional parameters are not known but they are significant. These results suggest that, in the film, framework distortions but also cation substitutions generated the "$2a_p \times 4a_p$" periodicity. In that way, the "$2a_p \times 4a_p$" structure can be compared with the $(Cu_{0.5}C_{0.5})Ba_2Ca_{n-1}Cu_nO_{2n+3}$.[10] However, it differs from the latter, by the nature of the alkaline earth which is solely Sr, by the C/Cu ratio of the carbonate layer which is likely superior to 1 and by the

(10) Alario-Franco, M. A.; Bordet, P.; Capponi, J. J.; Chaillout, C.; Chenavas, J.; Tournier, T.; Marezio, M.; Souletie, B.; Sulpice, A.; Tholence, J. L.; Colliex, C.; Argoud, R.; Baldonedo, J. L.; Gorius, M. F.; Perroux, M. *Physica C* **1994**, *231*, 103.

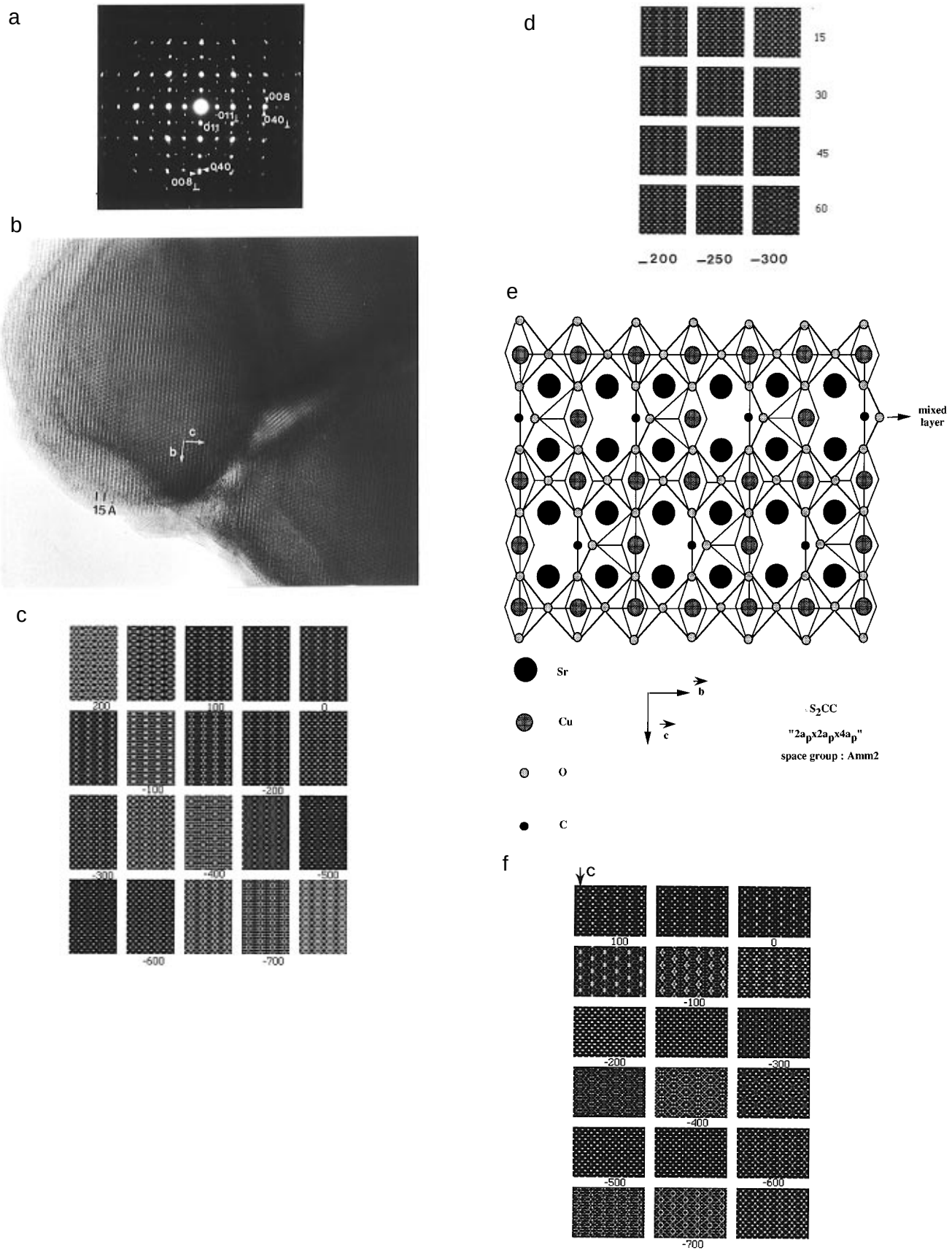

Figure 3. $Sr_2CuO_2CO_3$, second structural type. (a) [100] ED showing the structure "$2a_p \times 4a_p$" and the conditions limiting the reflection $0kl$, $k + l = 2n$. Two 90° oriented variants are superimposed. (b) Corresponding HREM image showing clearly the centered arrangement of the bright dots. (c) Calculated focus series for the "$2a_p \times 4a_p$" superstructure based on slight atomic displacements (positional parameters given in ref 8, space group $I\bar{4}$, and a thickness of 25 Å). (d) Calculated images for $\Delta f \approx -200$, -250, and -300 Å (horizontal) and a crystal thickness up to 60 Å (vertical). (e) Idealized structure of the "$2a_p \times 2a_p \times 4a_p$" superstructure resulting from the ordered substitution of one carbonate group out of two-by-one copper. (f) Calculated focus series of the "$2a_p \times 2a_p \times 4a_p$" superstructure for a thickness t of 45 Å (model in Figure 3e and space group $Amm2$).

$n = 1$ value which has not been observed in the Ba based series.

Nonstoichiometry: The two structures, "$a_p \times 2a_p$" and "$2a_p \times 4a_p$" behave very differently from the nonstoichiometry point of view.

The less defective is undoubtedly the "$2a_p \times 4a_p$" structure (Figure 3b). In a general way, we do not observe stacking defects so that one carbonate layer alternates very regularly with one copper layer. The only defects concern the ordering within the carbonate layer. In some areas, the centered contrast is not observed any more. Such a feature cannot be explained considering the I-type symmetry of this structure but is rather related to the existence of small domains with the "$a_p \times 2a_p$" structure. In the same way, local variations of the periodicity, along *b*, at the level of the carbonate layer can be easily explained in terms of Cu/C order−disorder phenomena.

The situation is different for the "$a_p \times 2a_p$" structure where various phenomena are observed. Viewing the overall HREM images (Figure 2b) shows two striking features. The first one deals with the small size of the oriented domains and the domain boundaries which are, as previously reported, mainly parallel to the $(001)_p$ or $(011)_p$ in a chevron-like pattern. The second point deals with the existence of stacking defects (a few defects are indicated by a white triangle and the number **1** in Figure 2b,c). At the level of these defects the carbonate layers are 11.4 Å spaced (instead of 7.5 Å), i.e., an additional perovskite layer is intercalated. In fact, it corresponds to the local formation of $Sr_3Cu_2O_{4+\delta}CO_3$ that is the member ($m = 1$, $n = 1$) of the family $(SrCuO_{2+\delta})_m(Sr_2CuO_2CO_3)_n$ (Figure 1b). These two features are by far, the most numerous in the film. Another important point is the local appearance of a $2a_p$ periodicity along *b* at the level of the carbonate rows. Some of these features are indicated by large black arrows in Figures 2b,c. In the enlarged image (Figure 2c) it clearly appears that it can be interpreted in terms of Cu/C substitution and ordering. When the phenomenon takes place over a very small areas (a few carbonate rows long) the periodicity along *c* remains close to 7.7 Å but as soon as it extends over a larger area the centered ordering is established and small areas of "$2a_p \times 4a_p$" structure are stabilized.

Other defects are sometimes observed. They are characterized by the formation of another stacking mode of the layers or by layer interconnections. An example is shown in Figure 2c, indicated by a small arrow in the left part of the image. The periodicity along *c* is locally close to 13 Å and a translation by $a_p/2$ of the cation position is observed along *b*. This is a well-known feature, usually observed in the Sr-based cuprates, which consists of the intercalation of one additional [Sr] layer, i.e., the local formation of a rock-salt-type layer. The connection of layers of different natures result from the existence of the stacking defects which are sometimes interrupted in the matrix. Some of them are indicated by **S** in the images. In these defects, the carbonate layers are directly connected to a copper layer and reciprocally, whereas the [SrO] layers become [Sr] layers (Figure 4a). A rare but interesting defect can be observed in the middle of Figure 2c (indicated by **C**). Two S_2CC slices (≈15 Å wide) are directly connected to a defective slice $Sr_4Cu_3O_{6+\delta}CO_3$ which is a member ($m = 2$, $n = 1$) where two carbonate layers are separated by three copper layers. Here again, the copper layers are connected to the carbonate layers through the junction but the [SrO] layers become [Sr] layers (Figure 4b).

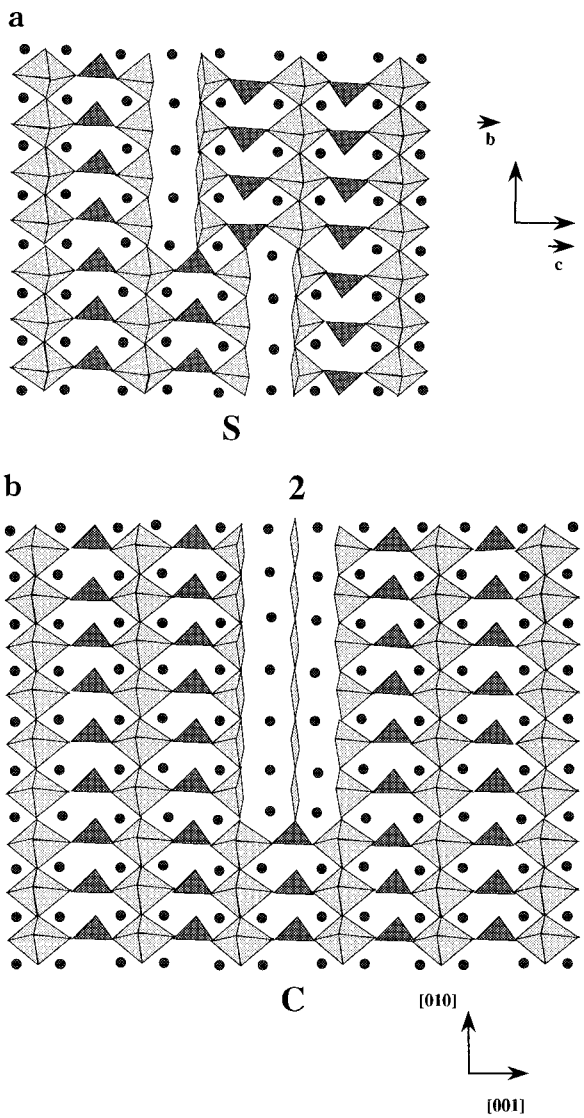

Figure 4. Idealized models of the defects marked (a) **S** and (b) **C**.

Film orientation: The *b* and *c* axes of the "$a_p \times 2a_p$" and "$2a_p \times 4a_p$" structures being parallel in the whole film, the directions of these two structures will be subscripted S2CC in this section, whereas those of the film will be superscripted NGO.

The ED patterns recorded in the thicker parts of the film show that the $[010]_{S2CC}$ and $[001]_{S2CC}$ directions of the oxycarbonate structure are parallel to the $[1\bar{1}0]_{NGO}$ and $[001]_{NGO}$ respectively.

The ED study demonstrates that in the film the oxycarbonates are *a*-axis oriented, i.e., the *a* axes of the structures are perpendicular to the substrate plane, so that they can be described as $[100]_p$ oriented with respect to an ideal cubic perovskite cell.

The relative orientations of the in-plane parameters of the substrate and of the two 90° oriented variants of the oxycarbonate are also very clear: (i) $[010]_{S2CC}$ or $[010]_p//[001]_{NGO}$ and $[001]_{S2CC}//[1\bar{1}0]_{NGO}$ for one domain; (ii) $[010]_{S2CC}$ or $[010]_p//[1\bar{1}0]_{NGO}$ and $[001]_{S2CC}//[001]_{NGO}$ for the 90° oriented domains.

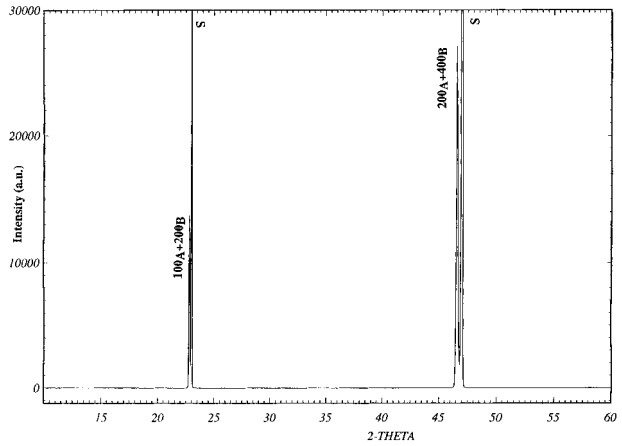

Figure 5. XRD pattern of $Sr_2CuO_2CO_3$ on $NdGaO_3$. A and B are respectively referred to the "$a_p \times 2a_p$" and the "$2a_p \times 4a_p$" structures. S indicates peaks of the substrate.

The sharpness of the reflections of the XRD pattern, given in Figure 5, confirms the high crystallinity of the film. The two diffraction peaks at $2\theta \approx 22.8°$ and 46.56° are consistent with the *a*-axis orientation observed by ED. They correspond to the 100 and 200 reflections of the "$a_p \times 2a_p$" structure and to the 200 and 400 reflections of the "$2a_p \times 4a_p$" structure so that *a* can be calculated to 3.9 or 7.80 Å, respectively.

These results show that the two types of $Sr_2CuO_2CO_3$ structures can be deposited in the form of thin film. The excess of copper evidenced by EDS analyses can also be easily explained. The first possibility is to stabilize a simple $Sr_2CuO_2CO_3$, with a "$a_p \times a_p \times 2a_p$" cell where $Sr_3Cu_2O_{4+\delta}CO_3$ members, (corresponding to $Sr_2Cu_{1.33}$) are intercalated. The second one is to partly substitute copper for carbon, forming $[C_{1-x}Cu_xO]$ layers which tend to be ordered.

Deposition of $Ba_{0.4}Sr_{1.6}CuO_2CO_3$ ($x = 1.6$). The ED pattern of this thin film (Figure 6a) shows that it is single phased. The most intense spots correspond again to the $a_p^* \times a_p^*$ mesh of the perovskite subcell but extra spots along the $[001]_p$ direction involve the tetragonal subcell $a \approx a_p$ and $c \approx 2a_p$. These parameters are in agreement with those observed in the bulk material $Ba_{0.5}Sr_{1.5}CuO_2CO_3$.[11] From these ED patterns, it clearly appears that, as observed for $x = 0$, there systematically exist 90° oriented variants so that the *b* and *c* axes of the oxycarbonate phase are parallel to $[001]_{NGO}$ and/or $[1\bar{1}0]_{NGO}$.

Consequently, the ED patterns show that the $x = 1.6$ thin film is also *a*-axis oriented, (i.e., $[100]_p$ oriented), and consists of 90° oriented domains with $b \approx a_p$ and $c \approx 2a_p$ axis lying in the plane of the film. They therefore exhibit the same orientation as the S_2CC film, i.e., parallel to the [001] and $[1\bar{1}0]$ directions.

The HREM images (Figure 6b) show that the film is well crystallized, and that the 90° oriented domains are almost similar to those observed in the $x = 0$ film. One can observe that the number of stacking defects decreases and that the short-range ordering phenomena at the level of the carbonate layers do not exist anymore. It should be noted that a few domains exhibit a different contrast where the carbonate rows are no longer observed (indicated by a small white triangle). In these domains, the contrast consists of a square array of bright dots 2.7 Å which is that expected for a *c*-axis oriented oxycarbonate structure.

(11) Armstrong, A. R.; Edwards, P. P. *J. Solid State Chem.* **1992**, *98*, 432.

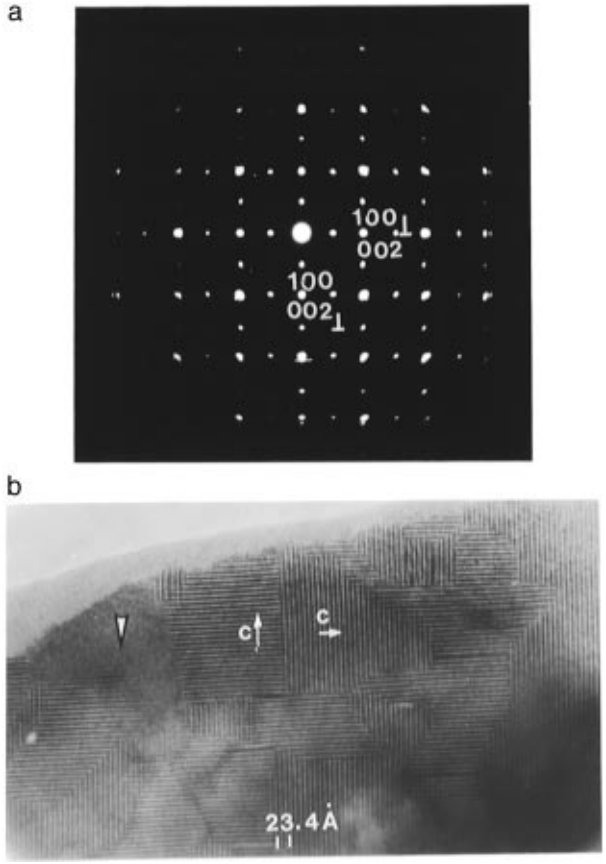

Figure 6. $Ba_{0.4}Sr_{1.6}CuO_2CO_3$. (a) ED pattern recorded along the direction perpendicular to the substrate. (b) Corresponding HREM image. The area marked by a small white triangle is *c*-oriented.

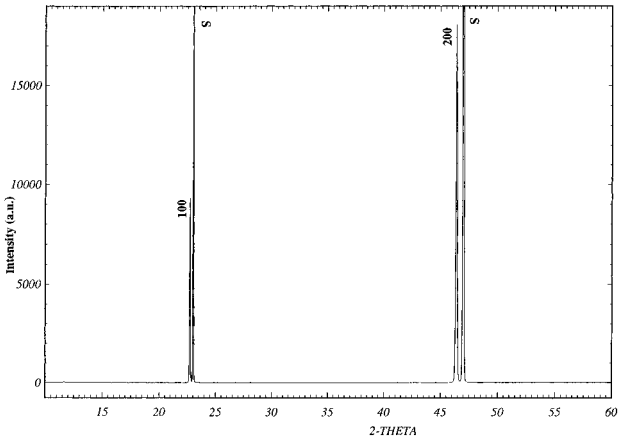

Figure 7. XRD pattern of $Ba_{0.4}Sr_{1.6}CuO_2CO_3$ on $NdGaO_3$. S indicates peaks of the substrate.

The XRD patterns (Figure 7) confirm the above observations. Two diffraction peaks are observed at $2\theta \approx 22.72°$ and 46.53°, corresponding to the 100 and 200 reflections respectively, leading to $a \approx 3.91$ Å.

In that way, the introduction of small amounts of barium ($x > 1.6$) in S_2CC, though it increases the symmetry of the structure, has no influence upon the orientation, leaving it *a*-axis (or $[100]_p$) oriented.

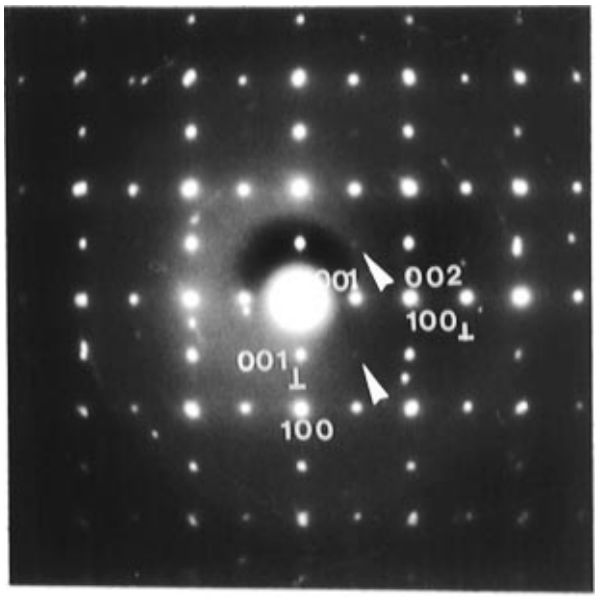

Figure 8. $Ba_{1.1}Sr_{0.9}CuO_2CO_3$: ED pattern recorded along a direction perpendicular to the substrate.

Deposition of $Ba_{1.1}Sr_{0.9}CuO_2CO_3$ ($x = 0.9$). For this composition, Kinoshita et al.[12] evidenced superconductivity at 40 K in the bulk material. Although the structural principle is maintained, the cell parameters determined on bulk samples are different from S_2CC and from $Ba_{0.4}Sr_{1.6}CuO_2CO_3$; the phase exhibits a double tetragonal cell, with $a \approx \sqrt{2}a_p$ and $c \approx 2a_p$.[10]

The ED pattern of the $x = 0.9$ film is displayed in Figure 8. It differs from that observed for $Ba_{0.4}Sr_{1.6}CuO_2CO_3$ (Figure 5) by the existence of very weak extra reflections (indicated by small white arrows). They result from the existence of small *c*-axis-oriented domains, as mentioned in the $x = 0.4$ film and correspond to the 100 and 010 reflections indexed in the double cell. The TEM images also evidence 90° oriented domains which appear to be larger than those observed for S_2CC and for $Ba_{0.4}Sr_{1.6}CuO_2CO_3$.

This shows that the structure has the same orientation with respect to the substrate as for the latter phases. As a consequence, the copper oxygen layers have the same orientation with respect to the substrate, i.e., their a_p parameter is perpendicular to the substrate plane. Thus, the film is [110] oriented with the following orientations within the plane of the substrate: $[1\bar{1}0]_{BSCC}$ or $[010]_p$//$[001]_{NGO}$ and $[001]_{BSCC}$//$[1\bar{1}0]_{NGO}$ for one domain; $[1\bar{1}0]_{BSCC}$ or $[010]_p$//$[1\bar{1}0]_{NGO}$ and $[001]_{BSCC}$//$[001]_{NGO}$ for the 90° oriented domains.

The XRD pattern confirms that the [110] direction is perpendicular to the substrate (Figure 9). Two peaks are observed at 22.56° and 46.06°, respectively. These can be indexed as the 110 and 220 reflections, showing a significant increase of the *a* parameter that is $a = 3.94$ Å.

These results show that the introduction of large amounts of barium ($x < 1.6$), on the strontium sites, changes the cell parameters of the structure but does not change its orientation with respect to the substrate, the $[CuO_2]_\infty$ layers remaining perpendicular to the substrate, so that the cell which is built on the diagonals of the tetragonal cell of $Ba_{0.4}Sr_{1.6}CuO_2CO_3$ ($a \approx \sqrt{2}a_p$ instead of a_p), is [110] oriented (corresponding to the same orientation of the perovskite subcell).

(12) Kinoshita, K.; Yamada, T. *Nature* **1992**, *357*, 313.

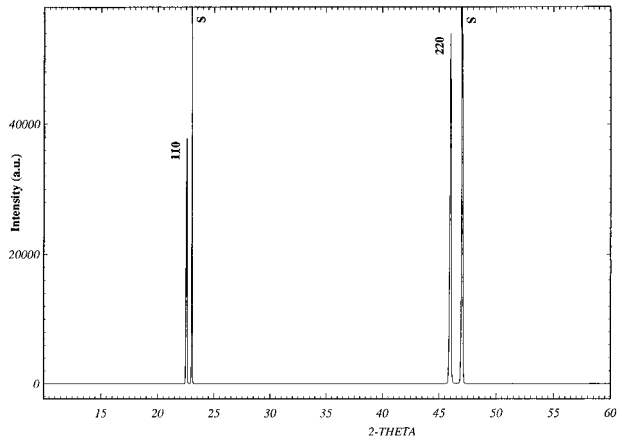

Figure 9. XRD pattern of $Ba_{1.1}Sr_{0.9}CuO_2CO_3$ on $NdGaO_3$. S indicates peaks of the substrate.

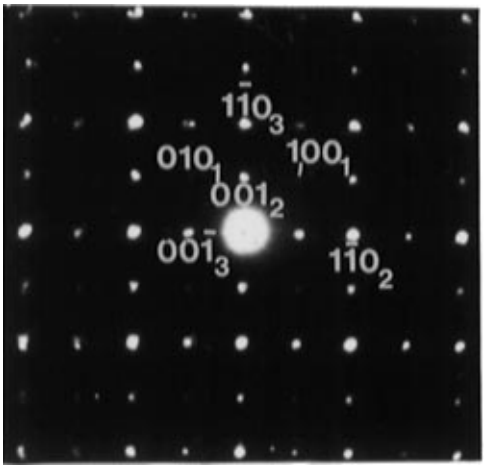

Figure 10. ED pattern of $Ba_{1.7}Sr_{0.3}CuO_2CO_3$ recorded along a direction perpendicular to the substrate. 1, 2, and 3 are respectively referred to the [001], [1$\bar{1}$0], and [110] orientation.

Deposition of $Ba_{1.7}Sr_{0.3}CuO_2CO_3$ ($x = 0.3$). For this composition, the parametric cell relationships with the perovskite do not change $a \approx \sqrt{2}a_p$ and $c \approx 2a_p$. Despite this great similarity, we previously found that for $x = 0.4$, $Ba_{1.6}Sr_{0.4}CuO_2CO_3$, three orientations of the structure coexist in the thin film with respect to the substrate.[5] In the different domains, either the [110], [1$\bar{1}$0], or [001] axes are perpendicular to the substrate plane.

To promote *c*-axis orientation, attempts were made to deposit thin films with a maximum barium content. Starting from a target with a composition "$Ba_{1.9}Sr_{0.1}CuO_3$", the EDS analyses show that the oxycarbonate phase of the film correspond to the cationic composition "$Ba_{1.7}Sr_{0.3}Cu$", i.e., the maximum *x* value is 0.3. This change of composition between the target and the film is not surprising for such a compound. It has already been reported by Nobumasa et al. for a Ba_2CuO_{3+y} target.[13]

The ED patterns of the $Ba_{1.7}Sr_{0.3}CuO_2CO_3$ (Figure 10) and $Ba_{1.6}Sr_{0.4}CuO_2CO_3$ phases are similar and show that three orientations of the structure exist in the film: [110], [1$\bar{1}$0], and [001].

(13) Nobumasa, H.; Horiuchi, K.; Shimizu, K.; Kawai, T. *Physica C* **1996**, *257*, 25.

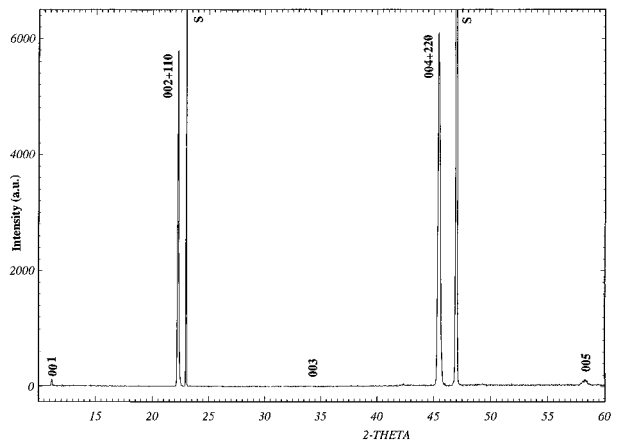

Figure 11. XRD pattern of $Ba_{1.7}Sr_{0.3}CuO_2CO_3$ on $NdGaO_3$. S indicates peaks of the substrate.

The XRD pattern (Figure 11) shows five peaks which are consistent with a lattice parameter of 7.9 Å. It is indeed not possible to detect the [110] orientation because the 002 and 110 reflections are at the same position (also the 004 and the 220), i.e., $d_{110} \approx d_{002}$ and $d_{220} \approx d_{004}$.

Concluding Remarks

This study shows that it is possible to deposit single-phase thin films of the $Ba_{2-x}Sr_xCuO_2CO_3$ oxycarbonates on $NdGaO_3$ substrate, by the pulsed laser deposition technique, with x ranging from 0.3 to 2.

Although an intergrowth of $Sr_2CuO_2CO_3$ and $SrCuO_2$ layers has been previously prepared as a thin film by postannealing in a CO_2/O_2 atmosphere,[14] it is the first time that the parent structure $Sr_2CuO_2CO_3$ has been deposited as a thin film. Moreover, one must emphasize that the nature of the substrate seems to play an important role, since attempts to deposit this phase on [110] $NdGaO_3$ substrates were unsuccessful except for one temperature of the substrate.

This study firstly shows that the growth of *c*-axis-oriented thin films is favored by increasing the barium content. One indeed observes that, at a temperature deposition of 680 °C, a very high barium content ($x \leq 0.4$) is necessary to induce the *c*-axis deposition. Nevertheless, it is not the only parameter since pure *c*-axis oriented thin films could not be obtained by only increasing the barium content. The temperature of the substrate should play an important role in this phenomenon. It has been shown that the orientation of $YBa_2Cu_3O_{7-\delta}$ thin films changes from *a*-axis to *c*-axis with increasing the substrate temperature[15] by a topotactic transformation.[16] In the oxycarbonate phases, the amplitude of the temperature variation is limited by the metastable character of the compounds, which decompose as soon as the temperature is increased above 710 °C. Note however that attempts to grow thin films of the phase $Ba_{1.6}Sr_{0.4}CuO_2CO_3$ at a higher temperature (720 °C) did not allow the *c*-axis oriented domains to be extended. In the same way, the growth at a lower temperature, 620 °C, did not allow the [110] oriented domains to be extended.

Another important point deals with the relationship between the film orientation and the mismatch between cell parameters of the $Ba_{2-x}Sr_xCuO_2CO_3$ films and the [110] oriented $NdGaO_3$ substrate. The mismatch can be calculated taking the a_p parameter of the cubic perovskite as a reference. For every phase, these parameters will be denoted a', b', and c':

(i) For the substrate $NdGaO_3$, the a'_{NGO} and c'_{NGO} parameters which correspond to the parameters in the plane of $NdGaO_3$ are

$$a'_{NGO} = \frac{\sqrt{a_{NGO}^2 + b_{NGO}^2}}{2} = 3.864 \text{ Å}$$

$$c' = c_{NGO}/2 = 3.853 \text{ Å}$$

(ii) For the $Ba_{2-x}Sr_xCuO_2CO_3$ phases, different relationships correspond to the different structures:

$$a' = a/2 \qquad c' = c/4 \text{ for } Sr_2CuO_2CO_3$$

$$a' = a \qquad c' = c/2 \text{ for } Ba_{0.4}Sr_{1.6}CuO_2CO_3$$

$$a' = a/\sqrt{2} \qquad c' = c/2 \text{ for } Ba_{1.1}Sr_{0.9}CuO_2CO_3 \text{ and } Ba_{1.6}Sr_{0.4}CuO_2CO_3$$

The mismatch, in percent, can be then defined for two different axis orientations.

For the *c*-axis thin films, the percent mismatch corresponds to

$$M(\%) = \frac{|2a' - a'_{NGO} - c'_{NGO}|}{a'_{NG_O} + c'_{NGO}} \times 100$$

For the *a*-axis-oriented thin films ([100] or [110] oriented films)

$$M(\%) = \frac{|a' + c' - a'_{NGO} - c'_{NGO}|}{a'_{NGO} + c'_{NGO}} \times 100$$

These parameters and percentage mismatch together with the film orientation are summarized in Table 1.

It appears that the [100] (or [110]) axis orientation, exhibits systematically the smaller mismatch compared to the [001] orientation, except for $Sr_2CuCO_3O_2$ for which the mismatches can be considered as very similar for both orientations. Moreover, one observes that for $Ba_{1.6}Sr_{0.4}CuO_2CO_3$ the mismatch for a [001] orientation is larger (3.45%) than for a [110] orientation of the film (2.77%) and also significantly larger than for a [001] orientation of $Ba_{1.1}Sr_{0.9}CuO_2CO_3$ (1.95%) so that the [110] orientation should be formed for $Ba_{1.6}Sr_{0.4}CuO_2CO_3$ contrary to these observations. In the same way, the oxycarbonate $Sr_2CuO_2CO_3$ that exhibits the smaller mismatch for the [001] orientation compared to all other phases and a similar mismatch for the [100] orientation (1.15%) should be the best candidate for a [001] orientation (0.86%), which has never been observed for this compound. Thus, these observations demonstrate that the lattice mismatch, which is often used for explaining the preferential axis orientation of $YBa_2Cu_3O_{7-\delta}$ thin

(14) Feenstra, R.; Budai, J. D.; Christen, D. K.; Kawai, T. *Appl. Phys. Lett.* **1995**, *67*, 1310.
(15) Hamet, J. F.; Mercey, B.; Hervieu, M.; Poullain, G.; Raveau, B. *Physica C* **1992**, *198*, 193.
(16) Hamet, J. F.; Blanc-Guilhon, B.; Taffin, A.; Mercey, B.; Hervieu, M.; Raveau, B. *Physica C* **1995**, *214*, 55.

Table 1. Lattice Mismatch between $Ba_{2-x}Sr_xCuO_2CO_3$ in the Bulk and $NdGaO_3$ at Room Temperature Calculated for an *a*-Axis and a *c*-Axis Thin Film[a]

	x			
	2	1.5	0.9	0.4
cell parameters *a′b′c′*	$2a_p \times 2a_p \times 4a_p$ and $a_p \times a_p \times 2a_p$	$a_p \times a_p \times 2a_p$	$\sqrt{2}a_p \times \sqrt{2}a_p \times 2a_p$	$\sqrt{2}a_p \times \sqrt{2}a_p \times 2a_p$
a′ (Å)	3.903 (7.806)	3.928 (3.928)	3.934 (5.564)	3.992 (5.645)
c′ (Å)	3.748 (14.993)	3.802 (7.604)	3.928 (7.856)	3.939 (7.878)
mismatch for a *c*-axis thin film *M* (%)	1.15	1.80	1.95	3.45
mismatch for an *a*-axis thin film *M* (%)	0.86	0.17	1.87	2.77
axis orientation with respect to the substrate plane of the thin film	$[100]_p$	$[100]_p$	$[100]_p$	$[100]_p + [001]$

[a] We indicate in parentheses the real value of the *a* and *c*. From refs 7, 11, 12, and 18.

films,[17] is not a prominent factor for the orientation of thin films of the oxycarbonates $Ba_{2-x}Sr_xCuO_2CO_3$. The fact that the mismatch is high, and consequently that the film growth does not correspond to a true epitaxy supports the point of view that the lattice mismatch does not influence strongly the growth orientation.

Several points such as the influence of the chemical reactivity and crystallographic behavior of barium upon the growth orientation, as well as the role played by the CO_2 and O_2 atmosphere, are so far not understood. Finally, it must be noticed that none of these films were found to be superconducting.

Nevertheless, these results will be used as a reference for the optimization of thin films of the superconductors $(CaCuO_2)_m(Ba_2CuO_2CO_3)_n$, eventually by doping with strontium, since this phase represents the first member of the series.

Acknowledgment. The authors acknowledge financial support from the human capital and mobility EEC network “Chemical synthesis of novel superconductors”.

CM960378P

(17) Jeschke, U.; Schneider, R.; Ulmer, G.; Linder, G. *Physica C* **1995**, *243*, 243.

(18) Armstrong, A. R.; Obhi, H. S.; Edwards, P. P. *J. Solid State Chem.* **1993**, *106*, 120.